Microstructural characterization and tribological behavior of Laser Furnace processed ceramic tiles

F. REY-GARCÍA [1,2], F. GUTIÉRREZ-MORA[3], C.J. BORREL[1], L.C. ESTEPA[1], L. A. ANGUREL[1], G. F. DE LA FUENTE[1]

1. Instituto de Ciencia de Materiales de Aragón, CSIC-Universidad de Zaragoza, María de Luna 3, E-50018 Zaragoza, Spain
2. Departamento de Física & I3N, Universidade de Aveiro, Campus de Santiago, 3810-193 Aveiro, Portugal
3. Dpto. De Física de la Materia Condensada, Facultad de Física, Universidad de Sevilla, Avenida de Reina Mercedes s/n, E-41012, Sevilla, Spain

CORRESPONDING AUTHOR:

Luis Alberto Angurel

Instituto de Ciencia de Materiales de Aragón (CSIC-Universidad de Zaragoza)

c/ María de Luna, 3

50018 Zaragoza (Spain)

e-mail address: angurel@unizar.es

Telephone: +34976762520

Microstructural characterization and tribological behavior of Laser Furnace processed ceramic tiles

F. REY-GARCÍA [1,2], F. GUTIÉRREZ-MORA[3]*, C.J. BORREL[1], L.C. ESTEPA[1], L. A. ANGUREL[1], G. F. DE LA FUENTE[1]*

1. Instituto de Ciencia de Materiales de Aragón, CSIC-Universidad de Zaragoza, María de Luna 3, E-50018 Zaragoza, Spain
2. Departamento de Física & I3N, Universidade de Aveiro, Campus de Santiago, 3810-193 Aveiro, Portugal
3. Dpto. De Física de la Materia Condensada, Facultad de Física, Universidad de Sevilla, Avenida de Reina Mercedes s/n, E-41012, Sevilla, Spain

*Authors to whom correspondence may be addressed: german.delafuente.leis@csic.es, fegumo@us.es

Abstract: This paper presents, for the first time, the processing of commercial ceramic tiles by means of Laser Furnace (LF) technology and its influence on their microstructure and tribology. Commercial porcelain and white clay, partially fired ceramic tiles, were processed by this method in order to study the effect of the laser treatment and its potential to produce ceramic items on a large scale, under extreme surface temperature conditions. The microstructure and depth of the laser irradiated ceramic samples were studied by FESEM. EDX analyses were employed to study composition before and after the laser treatment. Surface roughness was determined using Confocal Microscopy, while hardness and tribological behavior were studied using Vickers indentations and a ball-on-flat apparatus, respectively.

Key words: laser furnace, ceramic tile, porcelain tile, microstructure, hardness, wear

1 Introduction

Ceramic tiles are widely used as construction materials because of their outstanding mechanical properties and aesthetic appearance. These materials present good mechanical performance (high strength, hardness, toughness and abrasion resistance), chemical inertness (stain resistance) and an excellent aesthetic aspect (diverse decorative patterns and attractive matt or glossy finish) [1]. Essentially, tiles are made of clay, kaolin, feldspar and quartz [2, 3]. For most commercially available ceramic tiles, firing temperatures ranging between 1180ºC and 1240ºC are required to form a compact structure with crystalline phases embedded into a glass matrix [4]. The industrial fabrication of ceramic tiles is thus generally, although not exclusively, achieved by means of conventional, large gas roller furnaces [5] where a particular frit and glaze coating is integrated onto a clay substrate to give it specific properties. A variety of advanced functionalities have been demonstrated during recent years, by developing appropriate frit and glaze coatings [6] to fit particularly well onto each type of clay support.

Furthermore, when sintering temperature needs to be increased for achieving improved properties on the surface of the glazes, adjustment of the ceramic support composition is required in order to make compatible both, support and coating (frit and/or glaze). Moreover, alternative "natural" ceramic tiles are also part of the tile market, limited in surface finish and decoration, which may achieve improved mechanical properties when fired at temperatures approaching 1350 ºC. These are industrially produced with high quality and reliability. So is the case of classical porcelain, where pre-fired ceramic preforms are coated with high temperature pigments and glazes and finally sintered at temperatures ranging between 1400 and 1550 ºC, in what could be conveniently described as a double firing process [1, 3].

It would be desirable to access surface temperatures above those achieved nowadays in conventional ceramic sintering processes, because it is well known that, in many cases, the use of additives to extend and process glazes may deteriorate the mechanical properties expected from their pristine composition [7]. In addition, recent work on laser glazing of porcelain and alumina materials has demonstrated an attractive increase in surface hardness [8].

To our knowledge, the Laser Furnace (LF) method, based on a particular modification of the well-known Zone Melting method originally overviewed by Pfann in 1958 [9], is

the first scalable method to process ceramics continuously at extreme surface temperatures. These may well surpass the thermal limit of the substrate, thus invalidating the method for conventional furnaces. The LF method is based on a patent [10], especially applicable to process glass and ceramics with low thermal shock resistance. The sintering process is achieved using a continuous roller kiln and a defined temperature gradient inside the furnace, trying to obtain the same temperature profile already established for the conventionally sintered material. Simultaneously extreme temperatures are reached within the material's irradiated surface by employing a CO_2 laser, incorporated into the kiln and forming a horizontal line across the ceramic tile. This technology thus allows processing inorganic compound mixtures at relatively low average volume temperatures, compared to conventional processes, as well as its potential application at an industrial scale. In this regard, J. Llop [5] successfully processed forsterite coatings, from precursors deposited onto porcelain substrates, at 1150ºC by LF and at 1500ºC by conventional furnaces. Along the same line, ceramic tiles were successfully processed by continuously loading a LF prototype developed in the framework of the project CERAMGLASS, as reported by Fonseca et al. [11] with the objective of characterizing the associated particle emissions during the full ceramic firing cycle.

The selection and use of a high power CO_2 laser offers several advantages over alternative lasers. Its mid-IR (10.6 μm) emission wavelength is highly absorbed by most ceramic materials, regardless of color and composition, in contrast to alternative industrial nIR lasers emitting at wavelengths between 800 and 1100 nm. In addition, this laser may be combined with commercial galvanometer mirror units that enable high speed laser scanning and effective irradiation of large-areas [4, 5, 10-18].

The laser beam irradiation of a typical ceramic surface causes high temperature gradients in the vicinity of relatively small controlled melt volumes and promotes local, selective melting of the materials at their surface [13, 17-20]. The latter is combined with the thermal curve applied to the green ceramic substrate or tile, while it is at its highest volume temperature during the process (soaking phase). The result is a substantial reduction of temperature gradients between the solidification interface and the adjacent volumes within the ceramic body, yielding a significant reduction of micro-cracks associated to exaggerated thermo-mechanical stress [4, 16].

Recent advances published in the literature [4, 5, 11-18, 20-26] have demonstrated the advantages of the Laser Zone Melting (LZM) method to process thermal shock sensitive

materials, particularly with preheated substrates. Although Larrea and Mora had initially demonstrated the high degree of microstructural control provided by LZM [13, 14, 21-23], important improvements were later published, based on the use of preheating [4-5, 15-18, 24, 26] and novel optical beam maneuvering and sample translation devices [10].

The aim of this work is to study the application of the Laser Furnace method to the continuous fabrication and simultaneous surface treatment of industrial ceramic tiles. Microstructural and tribology characterization studies were carried out in order to explore the potential of the Laser Furnace method towards improving ceramic tile products, particularly by exposing them to extreme surface temperatures while maintaining their volume temperature at moderate values, in order to significantly reduce thermomechanical stresses.

2 Experimental

2.1 Laser treatment

This work has made use of partially fired, commercially available (Torrecid Group [27]), 10x10x0.4 cm white clay (PS samples) and porcelain (PL samples) ceramic tiles. Their compositions, provided by the supplier and reportedly measured by means of X-Ray Fluorescence (XRF), are summarized in Table I [27]. A laser treatment, similar to those described in ref. [4, 5, 10, 11, 15, 16] was applied by introducing samples in a laboratory scale (length = 4 m) Nanetti ER roller furnace, followed by focusing the beam of a pulsed 350W CO_2 laser (Rofin-Sinar Slab-type CO_2, UK), emitting at a wavelength of 10.6 μm, through ZnSe lens with 1100 mm focal length onto their surface (Fig. 1). The laser beam was directed through an optical beam steering system, which transformed the circular cross-section beam into a line measuring approx. 0.8 mm in thickness and 170 mm in width. The sample displacement rate was set in all experiments at 1.5 m/h. In order to avoid cracks, the temperature of the furnace was set in all cases to 650ºC, taking into account the porous state of the tile samples. Five samples of each type of tiles, porcelain and white clay, were laser furnace processed, changing the laser steering speed from 14.2 to 1416.7 cm/s. This modifies the fill factor, that is, the number of laser lines per sample displacement length, from 2 to 200 lines/mm.

The most relevant experimental parameters required to explain the effect of the laser treatment on the samples are summarized in Table II. For the calculation of the spot

laser fluence and spot irradiance values, it has been taken into account that the pulse width, in all cases, is 50 μs under a repetition rate of 20 kHz and a duty cycle of 50%. For these conditions, the energy per pulse at the maximum laser power is 17.5 mJ, and the incident laser spot during a pulse covers an area given by

$$A = \pi R^2 + 2R(v_l^2 + v_s^2)^{1/2} t \qquad \text{[Eq. 1]}$$

where R is the radius of the laser spot (0.4 mm), v_l is the laser beam scanning speed (perpendicular to sample displacement), v_s is the sample displacement speed, and t is the time that the laser is emitting during a pulse sequence, in the present case 25 μs. The second term of this formula is relevant at high laser beam scanning speeds (v_l), where laser spot displacement during each pulse may not be neglected. Besides these spot parameters, it is also important to consider how the energy is distributed on the irradiated surface. For this purpose, incubation energy, expressed in J/mm, has been introduced as an additional parameter. The latter has been calculated taking into account the number of pulses that are deposited on the material's surface per mm traversed. The values of these three parameters have been collected in Table II for the five experimental conditions established for this work.

2.2 Microstructural characterization

After processing the tiles through the Laser Furnace, small samples were prepared for SEM (Scanning Electron Microscopy) observation following the standard procedure developed to observe cross-sections [28]. Specimens were initially ground, mechanically polished and glued together in order to observe their cross-section profile.

Microstructural studies were performed using a Carl Zeiss MERLIN™ field emission scanning electron microscope (FESEM) operating at 15 kV, enabling observation with spatial resolution of 0.8 nm. Semi-quantitative elemental analyses were carried out with an INCA (Oxford) energy dispersive X-ray detector (EDX) coupled to the SEM unit and making use of an Oxford 350 analytical system.

The surface of the laser fired ceramic tiles was studied by Confocal Microscopy to determine the surface roughness and its relation to other properties and characteristics, such as texture and penetration depth, associated to the Laser Furnace treatment. A confocal microscope (Model 2300 PLμ, Sensofar, Spain) with a 10x objective (0.935 μm lateral resolution) was employed.

2.3 Mechanical and tribological characterization

Ceramic specimens of 3x3x0.4 cm^3 corresponding to white clay and porcelain tiles processed with low, intermediate and high spot fluence conditions were employed to carry out mechanical and tribological studies. Hardness tests were performed using a durometer (Struers Mod. Duramin, Ballerup, Denmark) using a Vickers indenter. Loads of 19.8 and 98 N during 20 s were used to perform the tests both in the laser-treated surface and in a plane perpendicular to the irradiated surface and away from it, for comparison purposes. At least 15 indentations were performed in each region for each sample. Wear behavior was studied using a tribometer (Microtest, Madrid, Spain) with a ball-on-flat configuration, employing alumina balls with normal loads of 1, 2, 5 and 10 N, and a sliding speed of 0.1 m/s for a distance of 500 m under ambient conditions of temperature and humidity. Alumina balls were selected so that certain similarities can be established with the well-accepted PEI (Product Enameler Institute) method, where gloss loss is measured in terms of the number of revolutions of steel balls and alumina powder in a wet environment [4]. Ball wear rates were determined from the radius of the circular scar left in the counterpart after the tests.

3 Results and discussion

3.1.- Changes in the microstructure and in the surface roughness induced by laser furnace treatments

SEM analysis, performed on polished and representative sample cross-sections, allowed to distinguish the influence of the laser treatment on each tile. The latter causes melting of the outermost surface, resulting in a compact, homogeneous and dense layer that seals the ceramic tile body [16, 29]. Figures 2-4 show the cross-sections of representative laser furnace processed ceramic tile samples obtained under fill factors of 2, 50 and 200 lines/mm. The corresponding pulse fluence, pulse irradiance and incubation energy values are reported in Table II.

As reported in previous literature work [4, 13, 29], the micrographs presented in Figures 2 to 4 show the three different zones that can be distinguished in the cross-section of laser treated samples. These include the lower, non-affected tile substrate, an intermediate heat-affected zone, and the molten-solidified outer layer (upper surface section). These are representative of all samples studied under different laser furnace

conditions, although the relative thickness of the intermediate zone and the outermost layer vary as a function of the imposed processing parameters.

Regarding the range of processing parameters used in this study, the dense, solidified outer layer exhibited thicknesses ranging between 179-202 μm (2 lines/mm fill factor, 3.46 J/cm^2 pulse fluence) and 9-17 μm (200 lines/mm fill factor, 2,23 J/cm^2 pulse fluence). The thickness values of this solidified region can be found in Table III for all the samples. A comparison between porcelain and white clay tiles allows identification of slight differences between them. A crossover behavior between both materials is observed as a function of the laser conditions imposed in the experiments. For low pulse fluence values, thicknesses measured in the porcelain samples are approximately 50% lower than in the white clay tiles. In contrast, with more intense laser conditions, the obtained thicknesses in the porcelain tiles are approximately a 10% higher. In order to understand this behavior, it is important to take into account that, although both tile types were originally fired at low temperatures, white clay tiles exhibit larger porosity than porcelain tiles. This may affect their response to laser irradiation, as it has been reported that porosity increases the level of laser absorption due to increased scattering [30]. As mentioned earlier, at low laser doses, corresponding to high beam scanning rates (50-200 lines/mm), thicker melt-solidified layers are observed in the case of white clay tiles, where porosity is higher than in porcelain tiles. Apparently, as the laser dose is increased, the porosity difference between both types of tiles does not seem to significantly influence the final dense surface layer attained after melting. Porosity is therefore an important parameter to take into account at low laser doses, when thin, dense surface layers are sought.

SEM micrographs also show an increase in the porosity in the inner part of the molten-solidified layer, especially for the porcelain tiles at low laser doses (Figures 3 (b) and 4 (b)). This is consistent with the observations reported by Lahoz et al. [31], regarding the melting behavior of white clay and porcelain tiles. These authors report that the melt pool volume increases with output laser power for white clay tiles, and that these melt more readily than their porcelain counterparts [31]. A comparison of the micrographs shown in the above Figures allows concluding that, in the case of white clay samples, the melt forms more readily and it fills more efficiently the voids near the surface of the porous tile, reducing its porosity level near the melt interface, as compared to similar, laser-treated porcelain samples.

Although thickness values in the range of hundreds of microns are usually found in most commercial glazed tiles, it was an objective of this study to determine the effect of laser surface melt-sealing while maintaining the original surface roughness, as required for a number of tile applications, particularly dealing with anti-slippery surfaces under wet conditions [27]. These surfaces are presently obtained by conventional machining and/or traditional glazing methods, which leave open porosity or do not offer the precision attained with laser methods not yet developed in this ceramic tile sector [32]. In this context, Figures 5 and 6 provide additional information in order to better understand the effect of laser treatment in the modification of the surface roughness and in the evolution of the porosity.

In this regard, images presented in Figures 2 and 5 show that low beam scanning rates and high pulse fluence values yield rather thick solidified layers, with low surface roughness and without the presence of open porosity. It is obvious from these micrographs that the white clay samples exhibit more and much larger diameter pores, a consequence of densification and of the observed higher porosity in these tile bodies. These inner pores should not influence the outer surface properties in a negative way, since they are below a depth of ca. 50 µm, such as not to be affected by staining, a significant problem in polished glazed tiles and, sometimes, even in conventionally processed tiles [32]. It is important to mention that the outer surface of the sample exhibits a homogeneous composition, demonstrating that the material has been completely melted in this section. This complete melting enabled an appreciable reduction in surface roughness.

In contrast, the behavior of samples processed at faster laser beam scanning rates and lower pulse fluence values (Figures 4 and 6) is different. In the case of the white clay tiles, the laser energy is not sufficient to melt all the phases that are present in the sample. The presence of large SiO_2 grains, characterized by darker grey contrast than the rest of the molten material, is thus observed in Figure 6. In some points, these grains reach the surface of the tile, increasing its roughness. Analyzing the behavior of the porcelain tile under these conditions, this layer is so thin that the surface roughness follows the trends of the original material. A similar behavior has been observed in the samples of both types of materials processed with 50, 100 and 200 lines/mm. Although these layers are very thin, the laser treatment was sufficient to close the open porosity at the surface of the tile, a much desired effect.

These effects of the laser furnace treatment on surface roughness have been confirmed using confocal microscopy. Ra values are collected in Table III and their change as a function of the laser fluence is presented for both types of tiles in Figure 7. Following the trends observed in SEM micrographs, it is clearly observed that roughness keeps nearly constant for low fluence values. In the case of the porcelain tiles, Ra values are very similar to those observed in the original material (ca. 10.3 μm). In contrast, and following the trends observed in Figure 6(a), white clay sample roughness values for laser treated samples are higher than those measured in the original sample (ca. 10.2 μm). Both materials show that above a certain fluence threshold, when the molten zone volume is sufficiently high, roughness starts to decrease. Values lower than 5 microns (Ra) are attained in the case of the porcelain tiles. This minimum is in the order of 10.8 microns for the white clay samples.

In addition, an important aspect of the present Laser Furnace process is that it enables, under optimum conditions, surface melting and resolidification while avoiding crack formation, as confirmed by the micrographs presented in this work. Crack formation is a problem in most laser melting treatments of ceramic materials, as demonstrated by Gutierrez-Mora et al. [4], who reported the presence of a large number of cracks in ceramic tile samples laser treated in similar fashion at room temperature.

An important aspect of the laser-material interaction deals with direct irradiance and pulse incubation effects, well described in the literature [19, 33-34]. In order to distinguish between these effects, graphical representations of how the laser furnace process parameters affect the solidified melt thickness at the tile surface are presented in Figure 8. The evolution of the melt thickness with the pulse fluence is initially presented in Figure 8 (a). A similar dependence is observed if the pulse irradiance is used in the analysis. It appears in the Figure that there is a threshold fluence value, above which a significant melt depth is attained. In addition, above this value of ca. 3.2 J/cm^2, the melt depth increases rapidly as a function of fluence. Thus it seems that a physical phenomenon is associated to this threshold value, consistent with the fact that absorption of laser light is sufficiently different between the solid and liquid surface irradiated [30, 35-36]. It appears here that, once a sufficient volume of liquid pool forms, absorption of laser radiation becomes more effective.

Incubation effects are observed, on the other hand, to be cumulative (Figure 8 (b)) and exhibit a pronounced effect on melt depth up to an incubation energy value of ca. 0.5 J/mm. After this value, the effect diminishes considerably, leveling off at values above

2 J/mm. As the scanning rate is decreased, the number of pulses per mm traveled by the tile surface under laser irradiation is increased accordingly. Such behavior is expected for processes where energy builds up progressively as the pulse repetition rate is increased, while maintaining all other process parameters constant. As the melt pool typically exhibits an inverted dome shape in ceramics [23] both, the depth and surface area of the melt pool increase, thus resulting in thicker solidified surface layers. This is exemplified in Figure 9 (a), where the typical melt pool induced by a CO_2 laser in an irradiated ceramic surface is illustrated. In addition, Figure 9 (b) illustrates the combination of laser pulses, which results in the affected layers observed by SEM and shown in Figures 2-6, and where an explanation for the depth leveling effect is suggested. Thus in Fig. 9 (b) the effect of increased pulses per mm gives rise to a melt with a similar depth, but increased volume reflected in a more extended area of the substrate surface. In essence, both higher irradiance and pulse repetition rate values lead to larger melt pools and, consequently, result in laser irradiated tiles exhibiting thicker surface layers. The thickness of the latter reaches a limit, however, at the expense of melt expansion along the tile surface.

Concerning the chemical composition of both types of tiles, white clay and porcelain, no compositional changes due to evaporation of component phases have been observed by EDX. Elemental analysis of the melt-solidified surface areas yields similar compositions to those of untreated tiles (Table I). It is thus plausible to conclude that the laser furnace process mainly affects (i) the densification of a surface layer, and (ii) the roughness of the tile surface, both to a degree largely determined by the laser irradiance and pulse incubation levels.

3.2.- Modifications in the mechanical and tribological behavior

To evaluate the mechanical behavior, samples treated with higher, medium and lower pulse fluences were selected and characterized using Vickers indentations. Results are collected in Table III. For comparison purposes, hardness measurements were also performed in regions away from the irradiation area, denominated as “bulk” in this Table. As mentioned above, high values of roughness were measured by confocal microscopy, suggesting that loads of 2 kgf (HV2 - 19.6 N) could only be applied to evaluate hardness on the smoother sample (PL1). When this load was applied to rougher samples, no definite shape of the indent was obtained, invalidating any determination of

hardness. In consequence, loads of 10 kgf (HV10 - 98.0 N) were used for the rest of the ceramic tile samples.

The values collected in Table III suggest that the bulk hardness of porcelain tile (PL) is much higher than that of white clay tile (PS). This is a logical result when taking into account the inherent porosity of the untreated samples.

On the one hand, analyzing the behavior of white clay tiles, the hardness is found similar in all samples, ca. 800-900 MPa regardless of the applied treatment, and similar to the values obtained for the bulk. On the other hand, in the case of the porcelain samples, an increase of the applied laser fluence enhances the hardness from 1160±90 MPa (PL5) to 1600±150 MPa (PL1). This variation in hardness can be explained when considering the nature of the coating; lower values for PL5 samples having to do with the porosity of the outermost surface layer. As it was noted before, SEM micrographs presented in Figures 2-6 show an increase in the porosity in the inner part of the molten-solidified layer, reducing the values of the measured hardness. PL1 shows hardness values similar to the bulk of untreated porcelain tiles, an observation associated to the load employed for the test (HV10). This is because at this load level, the affected material zone comprises both, the laser modified coating and the bulk. Besides, for this material, the surface roughness of the PL1 sample allows applying lower loads. Thus the hardness values obtained using a load of 2 kgf are significantly higher (4800±500MPa). With this load, only the region modified by the laser is affected, suggesting that this is the true value of the laser remelted surface hardness.

Figure 10 shows typical curves of the friction coefficient vs distance covered by the ball for all samples tested under an applied load of 5 N. In all plots a steady state is reached after a short running-in period. There appears to be a slight decrease in the friction coefficient with increasing laser fluence (Figure 10 (a)) for porcelain tiles, while no such trend is observed in white clay tiles (Figure 10 (b)). In porcelain tile samples, the coefficient of friction decreases, for this load, from 0.69 to 0.57 when the pulse fluence increases from 2.23 J/cm^2 (PL5) to 3.46 J/cm^2 (PL1). Data for all loads are gathered in Table IV, where the same trend is observed, namely, independence of the friction coefficient with pulse fluence for white clay tiles and lower friction coefficients as pulse fluence increases for porcelain tiles. The explanation for this trend seems to be related with the hardness of these materials. There is a direct correlation between friction coefficient and hardness. Hardness values for white clay tiles do not depend

significantly on laser pulse fluence, contrary to what is observed for porcelain tiles. This same trend is found for their friction coefficient values.

Figure 11 shows a series of wear tracks in tile samples, after friction tests using a 10 N load. As can be observed in the Figure, only a well-developed track was obtained for sample PL1 (Figure 11a). For the rest of tile samples, the tracks are not clearly observed. This behavior is related with the initial roughness of the samples. In Figures 11b, 11c and 11d it is shown that the wear damage depth is lower than the typical roughness parameters (Table III), making it impractical to determine the wear loss in the material. This Figure also indicates that the wear damage is concentrated in the laser modified layer, demonstrating that this layer is wear resistant and shows a firm cohesion to the bulk of the tile, since no delamination was observed in any of the worn tracks.

The fact that tested samples exhibit no well-developed worn tracks makes it very difficult to obtain a reliable wear resistance direct measure of the ceramic tiles studied. Thus, the wear of the ball has been estimated as an indirect measurement of the sample wear resistance. Ball wear rate data are also shown in Table IV.

Thus, the wear resistance of the ceramic samples was indirectly evaluated with the wear of the alumina ball employed in the experiments. For porcelain tile derived samples, the wear, normalized by distance (500m) and normal load, is very similar for all of the samples studied. This implies that the same wear mechanism is acting in all of the conditions applied to these samples. However, the ball wear rate for white clay ceramic tiles decreases with increasing fluence. For example, for 5N this parameter varies from 2.0 to 1.8 to 1.0 ($\times 10^{-4}$ mm^3/Nm) for samples when laser pulse fluence changes from 2.23 to 3.05 to 3.46 J/cm^2, respectively. Since hardness is similar in these samples, it can be assumed that the ball wear rate is directly related to surface roughness, taking this parameter values of 17.5, 15.7 and 10.8 μm, for the considered samples. Besides, the porcelain tile (PL) samples are more resistant to wear than those of white clay (PS) samples processed with the same fluence value (particularly for PL5 and PS5, see Table IV). One possible explanation for this trend has to do with the remnant porosity of the PS samples. This causes easier breakage of small particles from the tiles, which can act as a hard third body in the wear process. It is well known that third body abrasion increases the wear rate [37], as seems to be the case here.

According to the data shown in Table IV, no higher variations were observed in the friction coefficient for different specimens, ranging the most around 0.6. A general

tendency to increase the friction coefficient with the load may be observed. This fact can be related to a higher proportion of particles produced by the wear process at higher loads, where these act as a third body, increasing the friction coefficient.

Similar to hardness measurements, there is no clear trend observed associating the friction coefficient with the laser energy in laser furnace processed white clay tiles. However, it seems that there is an increase of the friction coefficient in porcelain samples when the laser energy is reduced. This coefficient increases when lower pulse fluence values are used. This behavior can be understood taking into account the decrease in hardness in these samples.

4 Conclusions

Porcelain and white clay commercial ceramic tiles have been treated by a patented Laser Furnace processing method. This method enables laser processing of surfaces at high temperatures, where thermal shock may be reduced conveniently in order to avoid excessive thermomechanical stress and microcrack formation. Both types of tiles were obtained with melt-solidified, dense surface layers, varying in thickness between 10 (at low irradiance values) and 200 μm (at high irradiance values) where open porosity was not observed and the original elemental composition was maintained throughout the process. Concerning their tribological behavior, the laser treatment does not significant affect white clay tiles. Porcelain ceramic tile hardness increases, however, when laser fluence is increased. The laser-modified surface layer retained its integrity, in both types of tiles, during wear tests. On the other hand, porcelain tile samples exhibit higher hardness values and wear resistance than their white clay counterparts.

Acknowledgements

Work supported under the auspices of Gobierno de Aragón/Fondo Social Europeo (Group T87, Laser Applications Laboratory and Group T12, Applied Superconductivity) and European Union through the CERAMGLASS Project under Grant LIFE11-ENV/ES/000560. F. Rey-García acknowledges the Portuguese Science and Technology Foundation (FCT) for the Grant SFRH/BPD/108581/2015. Authors acknowledge the use of Servicio General de Apoyo a la Investigación-SAI de la Universidad de Zaragoza.

References

[1] P. Escribano, J.B. Carda, E. Cordoncillo, Esmaltes y Pigmentos Cerámicos, in Enciclopedia Cerámica Vol. 1, Ed. Faenza Editrice Ibérica, Castellón, Spain, 2001.

[2] P.M.Tenorio Cavalcante, M. Dondi, G. Ercolani, G. Guarini, C. Melandri, M. Raimondo, E.R. Almendra, The influence of microstructure on the performance of white porcelain stoneware, Ceram. Int. 30 (2004) 953-963, https://doi.org/10.1016/j.ceramint.2003.11.002

[3] L. Sánchez-Muñoz, J.B. Carda, Materias primas y aditivos cerámicos, in Enciclopedia Cerámica. Vol. 2.1 (2002) and 2.2 (2003), Ed. Faenza Editrice Ibérica, Castellón, Spain.

[4] F. Gutiérrez-Mora, A. Domínguez-Rodríguez, V.V. Lennikov, G.F. de la Fuente, Influence of thermal effects produced by laser treatment on the tribological behavior of porcelain ceramic tiles. Key Eng. Mater. 423 (2010) 41-46, https://doi.org/10.4028/www.scientific.net/KEM.423.41

[5] J. Llop, Desarrollo de nuevas composiciones de gres porcelánico y estudio de su funcionalización a través de la tecnología láser, Ph.D. Thesis, Universitat Jaume I, Castellón, Spain, 2015.

[6] A.M. Berto, Ceramic tiles: above and beyond traditional applications, J. Eur. Ceram. Soc. 27 (2007) 1607-1613, https://doi.org/10.1016/j.jerceramsoc.2006.04.146

[7] L. E. Thiess, Influence of Glaze Composition on the Mechanical Strength of Electrical Porcelain, J. Am. Ceram. Soc. 19 (1936) 70-72, https://doi.org/10.1111/j.1151-2916.1936.tb19799.x

[8] R. M. Abdallah, I. M. Hammouda, M. Kamal, O. B. Abouelatta, A Abd. El-Salam, Evaluation of hardness, Surface Morphology and Structure of Laser Irradiated Ceramics, J. Ovonic Research, 6 (2010) 227-238.

[9] W.G. Pfann, (1958) Zone Melting, Chapman & Hall

[10] L.C. Estepa, D.F. de la Fuente, Continuous furnace with coupled laser for the surface treatment of materials, European Patent EP1992445 (2008), US Patent 20090230105 (2009), China Patent No. ZL 2012100224412 (2014).

[11] A.S. Fonseca, A. Maragkidou, M. Viana, X. Querol, K. Hämeri, I. de Francisco, L.C. Estepa, C.J. Borrell, V. Lennikov, G.F. de la Fuente, Process-generated nanoparticles from ceramic tile sintering: Emissions, exposure and environmental release, Sci. Total Environ. 565 (2016) 922-932, DOI: 10.1016/j.scitotenv.2016.01.106

[12] J. Bakali, E. Fortanet, G.F. de la Fuente, R. Lahoz, L.C. Estepa, G. Peris, I. Marinova, R. Pavlov, J.M. Pedra, J. Carda, Structural and microstructural characterisation of refractory oxides synthesised by laser, Key Eng. Mater. 264-26 (2004) 317-320, https://doi.org/10.4028/www.scientific.net/KEM.264-268.317

[13] A. Larrea, G.F. de la Fuente, R.I. Merino, V. Orera, ZrO_2-Al_2O_3 eutectic plates produced by laser zone melting, J. Eur. Ceram. Soc. 22 (2002) 191-198, https://doi.org/10.1016/S0955-2219(01)00279-5

[14] M. Mora, V.V. Lennikov, H. Amaveda, L.A. Angurel, G.F. de la Fuente, M.T. Bona, C. Mayoral, J.M. Andrés, J. Sánchez-Herencia, Fabrication of Superconducting Coatings on Structural Ceramic Tiles, IEEE Trans. Appl. Supercond. 19 (2009) 3041-3044

[15] I. de Francisco, V.V. Lennikov, J.A. Bea, A. Vegas, J.B. Carda, G.F. de la Fuente, In-situ laser synthesis of rare earth aluminate coatings in the system Ln-Al-O (Ln=Y, Gd), Solid State Sci. 13 (2011) 1813-1819.

[16] J. Gurauskis, V. Lennikov, G.F. de la Fuente, R.I. Merino, Laser-assisted, crack-free surface melting of large eutectic ceramic bodies, J. Eur. Ceram. Soc. 31 (2011) 1251-1256, https://doi.org/10.1016/j.jeurceramsoc.2010.08.017

[17] F. Rey-García, Planar Waveguides Obtained on Commercial Glass Substrates by Sol-gel and Laser Irradiation Methods, Ph.D. Thesis, Universidade de Santiago de Compostela, Spain, 2012.

[18] F. Rey-García, M.T. Flores-Arias, L.C. Estepa, W. Assenmacher, W. Mader, G.F. de la Fuente, Laser Zone Melting and Microstructure of Waveguide Coatings Obtained on Soda-Lime Glass, International Journal of Applied Glass Science 8 (2017) 329-336 DOI: 10.1111/ijag.12267

[19] H.G. Rubahn, Laser applications in surface science and technology, New York, Ed. John Wiley, 1999.

[20] E. Tejada-Rosales, S. Ondoño-Castillo, C. Diez, G.F. de la Fuente, N. Casañ-Pastor, Annealing of electrophoretic $YBa_2Cu_3O_7$ coatings on polycristaline substrates by zonal laser fusion, Bol. Soc. Esp. Cerám. V. 41 (2002) 185-189

[21] M. Mora, J.C. Diez, C.I. López-Gascón, E. Martínez, G.F. de la Fuente, Laser textured Bi-2212 in planar geometries, IEEE Trans. Appl. Supercon. 13 (2003) 3188-3191, https://doi.org/10.1109/TASC.2003.812192

[22] M. Mora, F. Gimeno, L.A. Angurel, G.F. de la Fuente, Laser zone melted $Bi_2Sr_2CaCu_2O_{8+\delta}$ thick films on (100) MgO substrate, Supercond. Sci. Technol. 14 (2004) 1133-1138, https://doi.org/10.1088/0953-2048/17/10/008

[23] M. Mora, C.I. López-Gascón, L.A. Angurel, G.F. de la Fuente, The influence of support temperature on Bi-2212 monoliths textured by diode laser zone melting, Supercond. Sci. Technol. 17 (2004) 1329-1334, https://doi.org/10.1088/0953-2048/17/11/015

[24] V.V. Lennikov, P.E. Kazin, Y.D. Tretyakov, G.F. de la Fuente, Laser zone melting and Texture Formation in MgO-doped BSCCO 2212, Z. Anorg. Allg. Chem. 630 (2004) 2337-2342, https://doi.org/10.1002/zaac.200400311

[25] A. Pascual, E. Fortanet, J.B. Carda, J.M. Pedra, R. Lahoz, G.F. de la Fuente, Ceramic tile decoration by laser technology. CFI-Ceramic Forum International 82 (2005) E37-E42.

[26] V.V. Lennikov, J.M. Pedra, J.J. Gómez, G.F. de la Fuente, J.B. Carda, In-situ synthesis of $MTiO_3$-Al_2O_3 composite coatings via Laser Zone Melting, Solid State Sci. 9 (2007) 404-409, https://doi.org/10.1016/j.solidstatesciences.2007.03.013

[27] Torrecid Group, S.A. www.torrecid.com

[28] S. Amelinckx, D. Van Dyck, J. Van Landuyt, G. Van Tendeloo, Electron Microscopy: Principles and Fundamentals, Weinheim Ed. Willey, 1997.

[29] Y.H. Ho, H.D. Vora, N.B. Dahotre, Laser surface modification of AZ31B Mg alloy for bio-wettability, J. Biomater. Appl. 29 (2015) 915-928, https://doi.org/10.1177/0885328214551156

[30] Lahoz, ‘‘Laser Ablation of Inorganic and Metallic Materials,’’ Ph.D. Thesis, University of Zaragoza, Zaragoza, 2006.

[31] R. Lahoz, G. F. de la Fuente, J. M. Pedra, J. B. Carda, Laser Engraving of Ceramic Tiles, Int. J. Appl. Ceram. Technol., 8 [5] 1208–1217 (2011) https://doi.org/10.1111/j.1744-7402.2010.02566.x

[32] H.J. Alves, M.R. Freitas, F.G. Melchiades, A.O. Boschi, Dependence of Surface porosity on the polishing depth of porcelain stoneware tiles, J. Eur. Ceram. Soc. 31 (2011) 665-671, https://doi.org/10.1016/j.jeurceramsoc.2010.11.028

[33] W. Steen, Laser Material Processing, Springer-Verlag: Berlin, 1991.

[34] P. Schaaf, ed. Laser Processing of Materials, Springer Series in Materials Science 139, Springer-Verlag, Berlin (2010).

[35] Petrov, Abrupt Increase of the Absorption Coefficient of Alumina at Melting by Laser Radiation and Its Decrease at Solidification, V.A. Int J Thermophys 30 (2009) 1938. https://doi.org/10.1007/s10765-009-0678-z.

[36] J. Lawrence, L. Li, Determination of the absorption length of CO_2 and high power diode laser radiation for a high volume alumina-based refractory material, Applied Surface Science 168 (2000) 71-74, https://doi.org/10.1016/S0169-4332(00)00593-6

[37] T. El-Raghy, P. Blau, M.W. Barsoum, Effect of grain size on friction and wear behavior of Ti_3SiC_2, Wear 238 (2000) 125-130, https://doi.org/10.1016/S0043-1648(99)00348-8

FIGURES

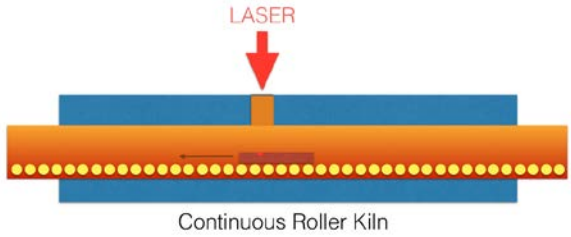

Figure 1: Simplified illustration of the Laser Furnace system employed to thermally process the white clay and porcelain tile samples reported in this study. The essential elements of the system include a CO_2 Laser emitting in pulse mode at 10.6 µm, an opening on the upper part of the kiln, and a continuous, three zone roller kiln, where tiles are transported at constant speed. The general Laser Furnace process is described in reference 10.

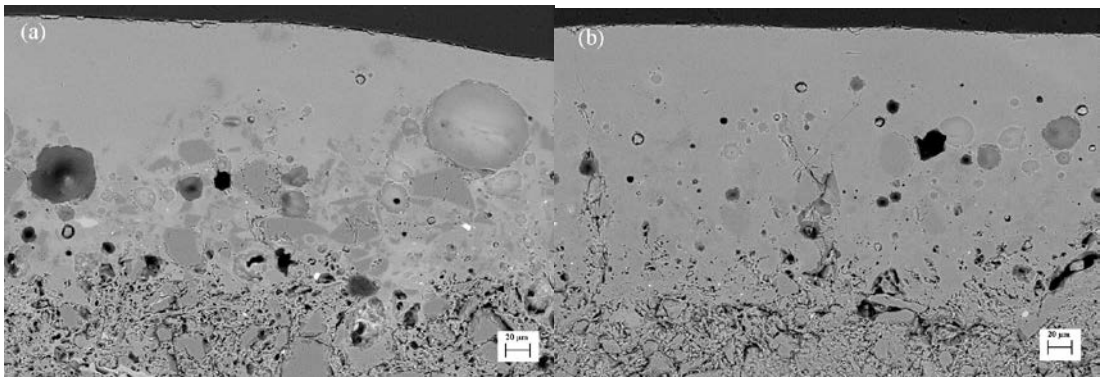

Figure 2: SEM micrograph of the cross-section of the samples treated with a fill factor of 2 mm/s (fluence value of 3.46 J/cm^2): (a) white clay tile, PS1, and (b) porcelain tile, PL1.

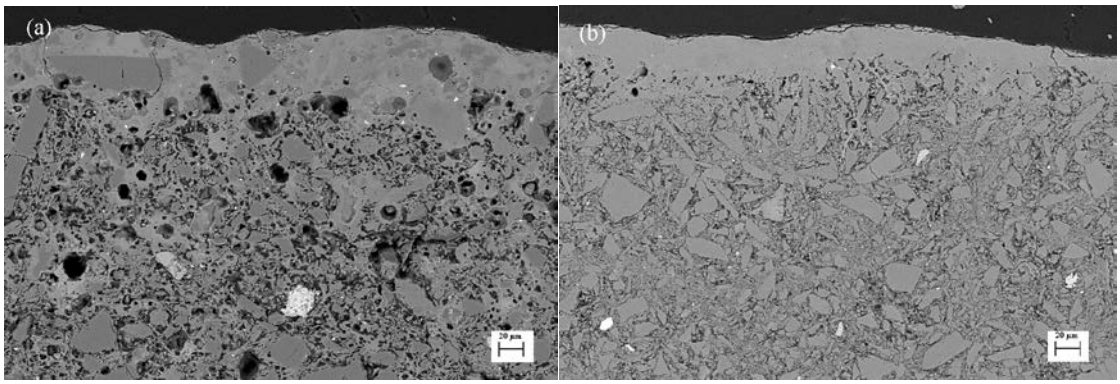

Figure 3. SEM micrograph of the cross-section of the samples treated with a fill factor of 50 mm/s (fluence value of 3.05 J/cm^2): (a) white clay tile, PS3, and (b) porcelain tile, PL3.

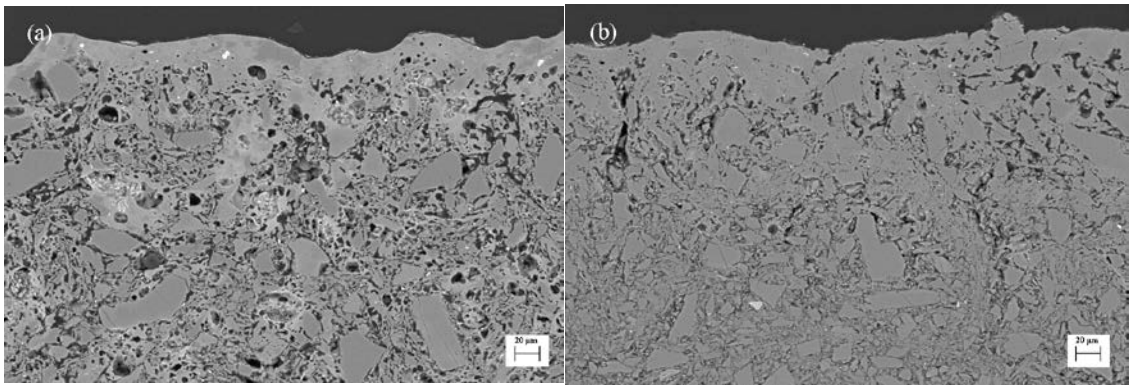

Figure 4. SEM micrograph of the cross-section of the samples treated with a fill factor of 200 mm/s (fluence value of 2.23 J/cm^2): (a) white clay tile, PS5, and (b) porcelain tile, PL5.

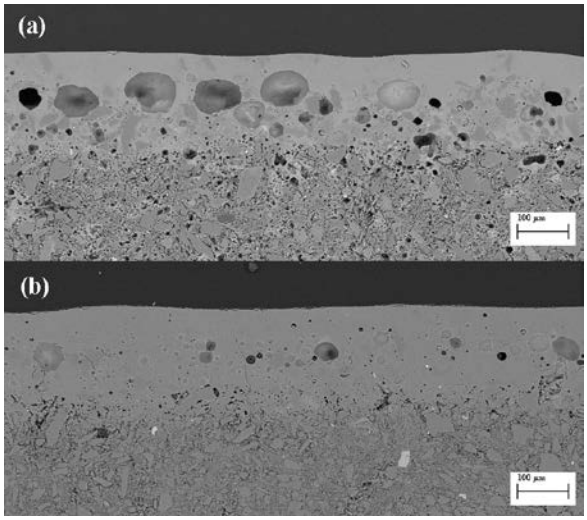

Figure 5. SEM micrographs obtained on cross sections, perpendicular to sample advancement, of the samples treated with a fill factor of 2 mm/s (fluence value of 3.46 J/cm^2): ((a) white clay tile, PS1, and (b) porcelain tile, PL1) illustrating the differences found in porosity and in surface roughness after laser furnace processing.

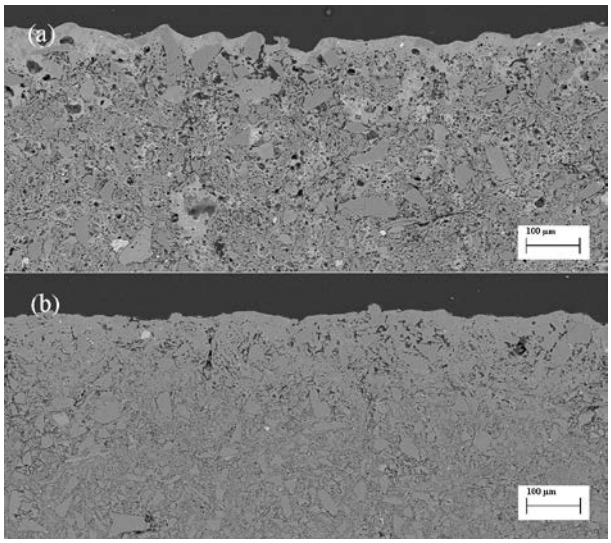

Figure 6. SEM micrographs obtained on cross sections, perpendicular to sample advancement, of the samples treated with a fill factor of 200 mm/s (fluence value of 2.23 J/cm^2): ((a) white clay tile, PS5, and (b) porcelain tile, PL5) illustrating the differences found in porosity and in surface roughness after laser furnace processing.

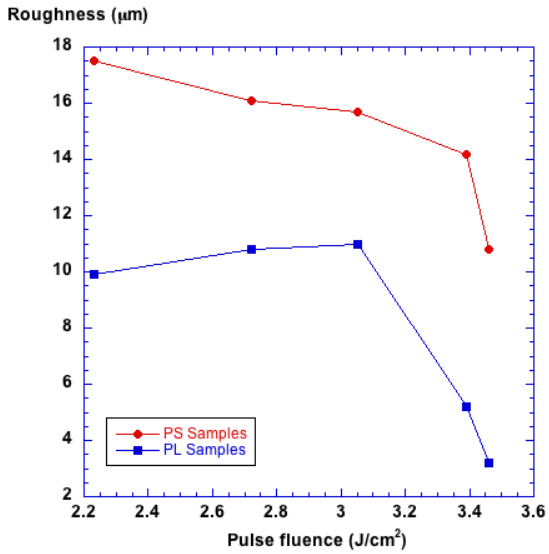

Figure 7: Evolution of the surface roughness parameter Ra with the laser fluence used in the treatment for white clay (red) and porcelain (blue) tiles.

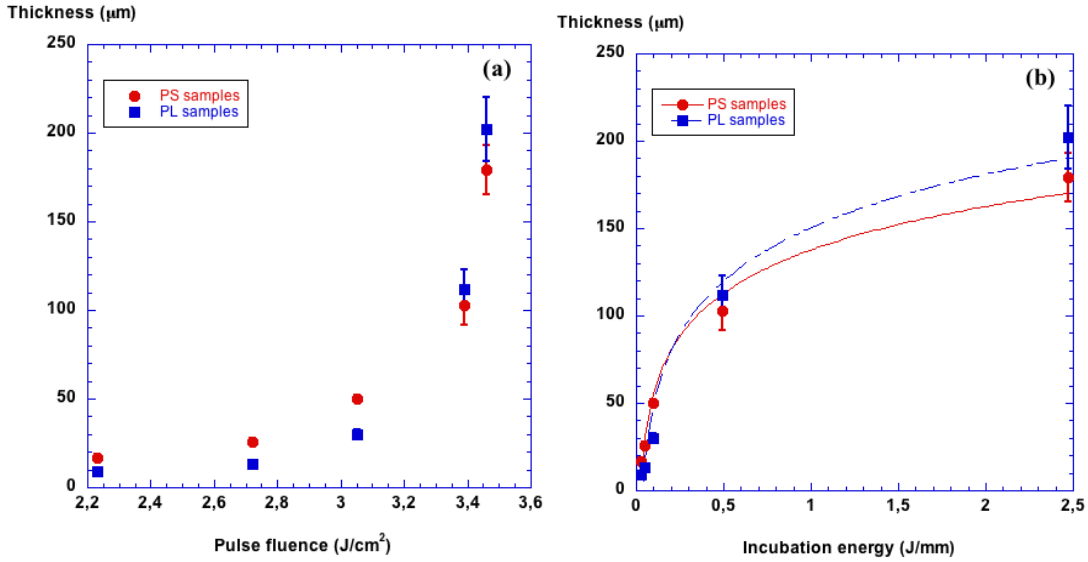

Figure 8. Laser Furnace molten-solidified surface layer thickness as a function of the following laser parameters: Pulse fluence (a), and Incubation energy (b). In this case, lines are fits to a logarithmic dependence.

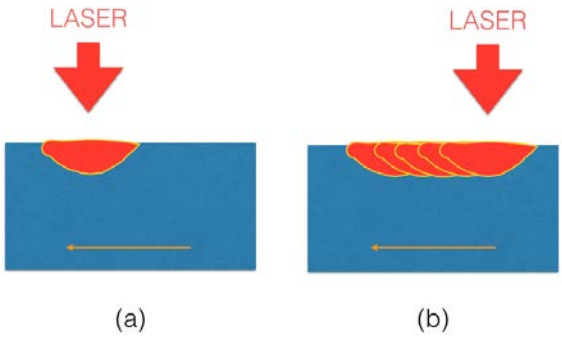

Figure 9. (a) Illustration of a typical melt pool induced by a CO_2 laser in an irradiated ceramic surface, where an inverted dome shape is related to the presence of liquid in the proximity of the laser incident spot; (b) representation of the combination of laser pulses, which results in the affected layers observed by SEM.

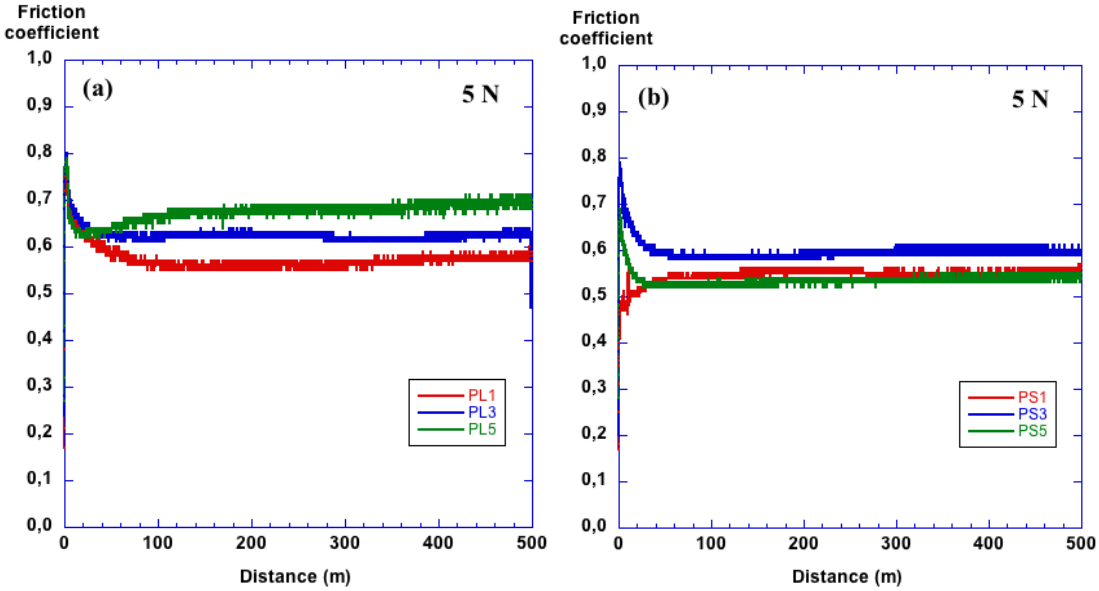

Figure 10: Friction coefficient vs distance covered by the alumina ball for different samples tested under 5N. a) Porcelain tiles and b) white clay tiles.

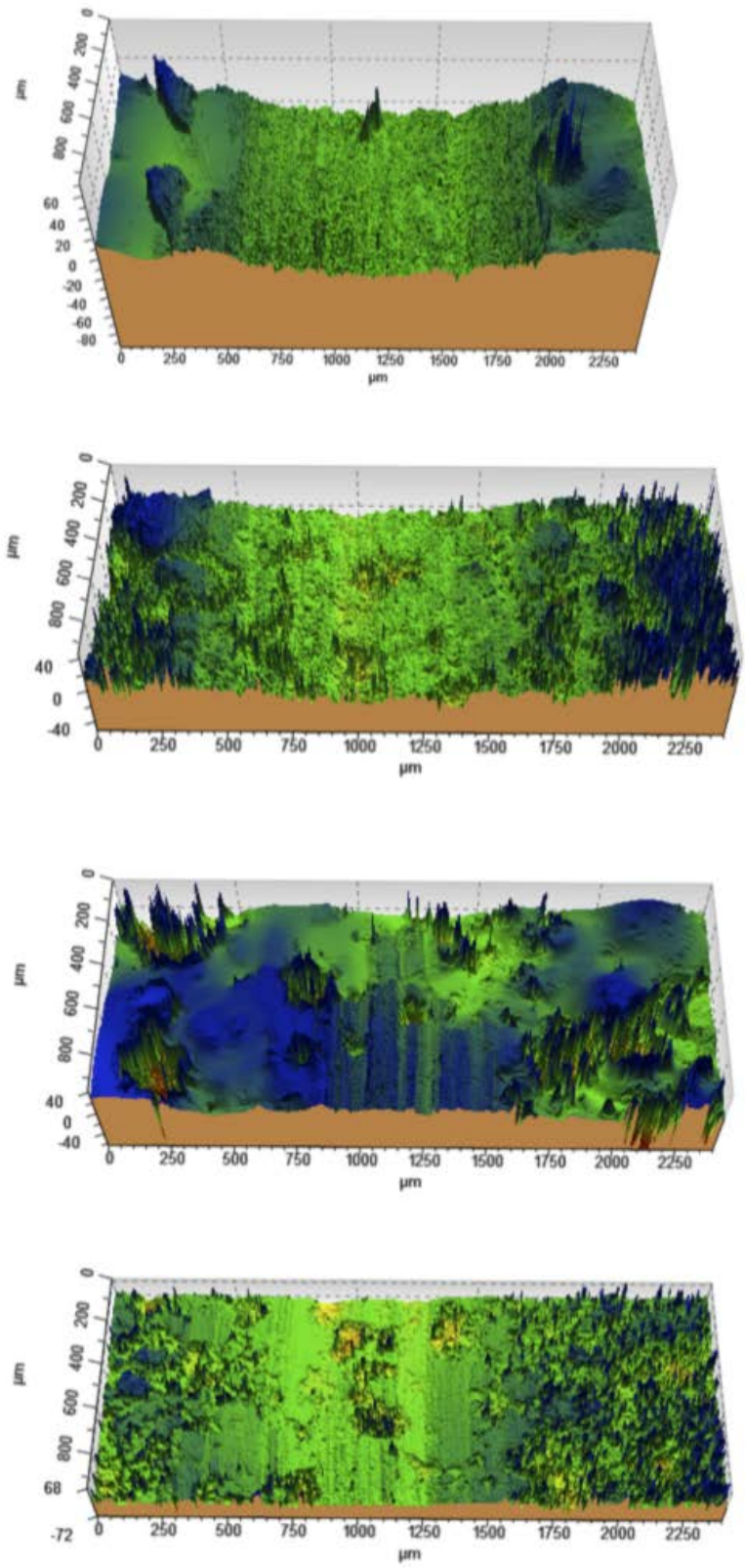

Figure 11: Confocal images of tile surface after wear tests using 10N: a) PL1, b) PL5, c) PS1, and d) PS5

TABLES

Table I: Main components of commercially available ceramic tiles, in %wt, obtained by X-ray fluorescence (XRF) and provided by Torrecid Group [27].

Oxide	*White clay porous tiles*	*Porcelain tiles*
SiO_2	63,05	70,19
Al_2O_3	16,10	18,61
Na_2O	0,44	5,53
K_2O	1,90	0,63
MgO	0,15	0,31
CaO	6,12	0,10
TiO_2	0,41	0,26
Fe_2O_3	1,46	0,22

Table II: Laser processing parameters applied during laser furnace treatments of porcelain and white clay porous tiles.

Fill factor (lines/mm)	Beam scan rate (mm/s)	Area irradiated/ pulse (mm^2)	Spot fluence (J/cm^2)	Spot irradiance (kW/cm^2)	Incubation energy (J/mm)
2	141,7	0,505	3,46	138,48	2,471
10	708,3	0,517	3,39	135,44	0,494
50	3541,8	0,573	3,05	122,06	0,099
100	7083,5	0,644	2,72	108,64	0,049
200	14167	0,786	2,23	89,06	0,025

Table III: Laser-affected thickness, roughness and hardness with a load of 10 kg of the different samples.

Sample	Fill Factor (lines/mm)	Avg Thickness (µm)	Roughness Ra (µm)	Hardness HV10 (MPa)
White clay				
Bulk				880±120
PS1	2	179±14	10.8	810±120
PS2	10	112±11	14.2	
PS3	50	32±2	15.7	860±70
PS4	100	26±2	16.1	
PS5	200	17±2	17.5	840±80
Porcelain				
Bulk				1640±150
PL1	2	202±18	4.3	1600±150
PL2	10	103±11	7.8	
PL3	50	30±3	12.5	1390±140
PL4	100	13±1	10.3	
PL5	200	9±1	9.9	1160±90

Table IV. Summary of measured friction coefficients and ball wear rates.

Sample		**PL1**	**PL3**	**PL5**	**PS1**	**PS3**	**PS5**
Friction coefficient (±0.05)	1N	0.42	0.44	0.56	0.54	-	0.28
	2N	0.58	0.48	0.63	0.51	0.52	0.45
	5N	0.57	0.62	0.69	0.53	0.59	0.53
	10N	0.58	0.60	0.68	0.65	0.59	0.63
Ball wear rate ($x10^{-4}$ mm^3/Nm) (±0.1)	1N	2.7	0.87	1.9	2.0	1.6	2.5
	2N	3.2	1.5	1.8	1.6	2.6	2.9
	5N	1.4	1.7	1.6	1.0	1.8	2.0
	10N	1.9	-	-	1.4	1.4	2.0